Plasmonic enhancement of spatial dispersion effects in prism coupler experiments

Armel Pitelet, Emilien Mallet, Rabih Ajib, Caroline Lemaître, Emmanuel Centeno, and Antoine Moreau*
Université Clermont Auvergne, CNRS, Institut Pascal, 63000 Clermont-Ferrand, France

(Received 25 April 2018; revised manuscript received 7 August 2018; published 21 September 2018)

Recent experiments with film-coupled nanoparticles suggest that the impact of spatial dispersion is enhanced in plasmonic structures where high wave-vector guided modes are excited. More advanced descriptions of the optical response of metals than Drude's are thus probably necessary in plasmonics. We show that even in classical prism coupler experiments, the plasmonic enhancement of spatial dispersion can be leveraged to make such experiments two orders of magnitude more sensitive. The realistic multilayered structures involved rely on layers that are thick enough to rule our any other phenomenon as the spill-out. Optical evanescent excitation of plasmonic wave guides using prism couplers thus constitutes an ideal platform to study spatial dispersion.

DOI: 10.1103/PhysRevB.98.125418

Spatial dispersion, i.e., the dependency of the permittivity on the wave vector, arises in metals because of the repulsive interaction between the free electrons inside the jellium. This phenomenon puts a limit to the validity of Drude's model [1], which has proven extremely accurate in plasmonics for more than a century now. This success can be related to the fact that Drude's model is the zeroth-order term of all the more advanced descriptions of the free-electron gas [2–6]. The first-order correction to the model, however, is intrinsically nonlocal: because of the repulsion between free electrons, the metal can still be described using an effective polarization, but the polarization in a given point depends on the electric field in the surroundings—at a typical distance close to the free mean path of the electrons.

The idea that spatial dispersion could have an impact on the optical response of metals and on surface plasmons dates back to the 1960s. Very advanced models [3,7], including the hydrodynamic model [2,4], were proposed at the time to tackle the problem. However, it became clear in the 1980s that no optical experiment with noble metals could show an impact of spatial dispersion large enough to threaten the predominance of Drude's model in plasmonics with an optical excitation. While spatial dispersion and more advanced models for surface plasmons [8–10] continued to be thoroughly studied in surface science, especially using EELS [11–13], the consensus seemed to be that Drude's model is largely sufficient in plasmonics [5,14].

For many in this community, the experiments showing Drude's model failure with large enough nanoparticles excited optically [15,16] thus came as a surprise. These experiments renewed the interest paid to the hydrodynamic model [17], which can be made accurate enough, provided the main parameter of the model is correctly chosen. In addition, they showed that small gaps between metals were able to largely enhance spatial dispersion, instead of relying on tiny particles [18,19]. However, the subnanometer gaps required to observe the impact of spatial dispersion raised some skepticism [20], all the more so that, in that case, the effects studied in surface science, like the spill-out, are likely to intervene strongly [21–23]. A lot of work has subsequently been devoted to (i) study theoretically in which situations spatial dispersion is likely to have an impact [24–27], (ii) develop numerical tools based on the hydrodynamical model [28–30] to accurately predict these effects in complex geometries, and, finally, (iii) to better understand the fundamental reasons why the hydrodynamic model, while it presents well-documented deficiencies [31], is able to take the impact of spatial dispersion into account correctly for noble metals [32,33].

In plasmonics, it is usually considered desirable to miniaturize structures to deeply subwavelength levels [34,35], which leads to a concentration of the fields in tiny volumes and to various exotic effects [36]. Such a feature can be achieved only with metals because, when light propagates in the vicinity of a jellium, it is slowed down—which generally means it acquires a much higher wave vector, a much smaller effective wavelength, and thus a much shorter typical variation length for the fields. When the effective wavelength decreases, it begins to approach the mean free path of electrons inside the jellium so that the local description, which assumes the current in a given point is determined by the electric field in the same point, can no longer be considered accurate. The slower the light, the smaller the typical scale of the field variation, and thus the higher the impact of spatial dispersion [26].

Here we propose to use the classical prism-coupler configuration [10,37] to excite high wave-vector plasmonic modes to enhance the effects of spatial dispersion alone. We predict, relying on the hydrodynamic model and accurate material parameters, that the impact of spatial dispersion will be two orders of magnitude larger than what can be reached with simple surface plasmons. The plasmonic resonances excited can be linked to the excitation of gap plasmons (GPs) [26,38], long-range surface plasmons (LRSPs) and short-range surface plasmons (SRSPs) [19,39–41], supported by multilayered structures with dimensions that are large enough to exclude other phenomenon like the spill-out [23]. Were such

*antoine.moreau@uca.fr

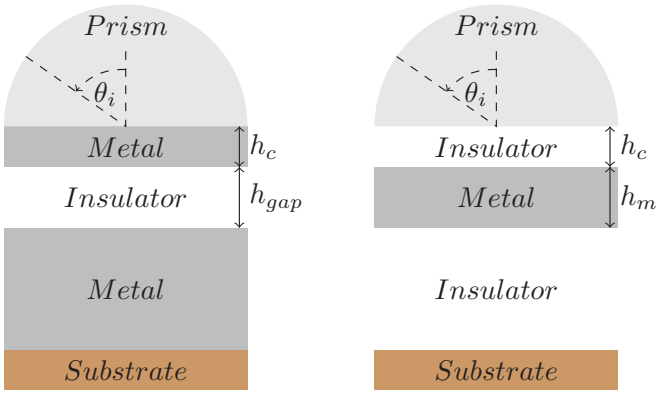

(a) MIM **(b)** IMI

FIG. 1. Schematic representation of the prism couplers: (a) resembles the Otto configuration, i.e., a prism on top of a metallic slab, which ensures coupling to the gap plasmon, while (b) resembles the Kretschmann-Raether configuration, i.e., a prism on top of a dielectric layer through which the guided modes of an IMI structure are coupled.

experiments to be conducted, they should allow to estimate the central parameter of the hydrodynamic model.

Figure 1 shows the prism-coupler structures for which the coupling condition can be written as a relation between the effective index $n_{\text{eff}} = k_x/k_0$ of a guided mode (characterized by a wave vector k_x at a frequency $\omega = k_0 c$) to the prism index n_p and angle of incidence at the prism bottom interface θ_i:

$$n_{\text{eff}} = n_p \sin(\theta_i). \tag{1}$$

Showing it is a way to measure the wave vector directly. Any change in k_x induced by spatial dispersion leads to a discrepancy between the coupling angle predicted using Drude's model and taking nonlocality into account. We underline, however, as will be clear in the following, that the change in the coupling angle is not the only change brought by nonlocality.

In the hydrodynamic model [5,17,26,32,33], the link the electric field $\mathbf{E}$ in the metal to the induced electronic current $\mathbf{J}$ is written as

$$-\beta^2 \nabla(\nabla \cdot \mathbf{J}) + \ddot{\mathbf{J}} + \gamma \dot{\mathbf{J}} = \epsilon_0 \omega_p^2 \dot{\mathbf{E}}, \tag{2}$$

ω_p being the plasma frequency, ϵ_0 the vacuum permittivity, and β the nonlocal parameter which describe the interactions between free electrons in metal. A special attention must be paid to (i) the material parameters—since our version of the hydrodynamic model makes an explicit distinction between the response of free electrons, considered as nonlocal, and the response of core electrons, considered as purely local—and (ii) the necessary additional boundary condition—here we impose that no electron is allowed to leave the metal. We underline that this condition is accurate only when the extraction work of the considered metal is high enough—which is the case only for noble metals [32], a well-known deficiency of the model.

For the material parameters, we rely on a Brendel-Bormann model that has been proven to be particularly accurate [42]. Finally, regarding parameters, several theoretical expressions exist for the nonlocal parameter β. We use a value of $\beta = 1.35 \times 10^6$ m $\cdot$ s^{-1} coming from the only experimental data currently available [16]. We underline that there two main theoretical expressions for β, and that the actual estimated value, coming from fits of the experimental data, is intermediate between the two. We use this value to estimate the enhancement of spatial dispersion in a given structure, but we stress that the setups we propose actually constitute a way to estimate this parameter too.

The reflectance of the structures is computed using Moosh, an open code [43] that is able to take spatial dispersion into account in the framework of the hydrodynamic model through the use of a specifically designed scattering matrix algorithm [29]. The situations described below result from a choice of the geometrical parameters which maximizes the impact of spatial dispersion—but the phenomenon is always easy to spot.

We first study the optical excitation of a GP resonance in a gap formed by an insulator layer sandwiched between two metallic slabs [see Fig. 1(a), MIM structure]. For the GP propagating in a dielectric layer with a permittivity ϵ_d between two metals with a permittivity $\epsilon_m = 1 + \chi_f + \chi_b$, where χ_f and χ_b are the susceptibilities linked to the free and bound electrons, respectively, the dispersion relation for a mode at frequency ω and with a wave vector k_x can be written [19,26]:

$$\frac{\kappa_d}{\epsilon_d} \tanh \frac{\kappa_d h}{2} + \frac{\kappa_m}{\epsilon_m} = \Omega, \tag{3}$$

where $\kappa_i = \sqrt{k_x^2 - \epsilon_i k_0^2}$ with $i = d, m$, $k_0 = \omega/c$, and $\Omega = \frac{k_x^2}{\kappa_l}\left(\frac{1}{\epsilon_m} - \frac{1}{1+\chi_b}\right)$ with $\kappa_l^2 = k_x^2 + \frac{\omega_p^2}{\beta^2}\left(\frac{1}{\chi_f} + \frac{1}{\chi_b}\right)$. The parameter Ω vanishes when there is no spatial dispersion, but increases with k_x, which leads to expect a larger impact for higher wave vector. The wave vector increases when h decreases, so that decreasing h leads to a higher discrepancy between Drude's model and the hydrodynamic model.

The effective index of the GP is controlled by the thickness of the dielectric h_{gap} supporting it [38]. As h_{gap} decreases, the wave vector of the GP increases and even diverges when $h_{\text{gap}} \to 0$. For an ultra-thin h_{gap}, the GP wave vector is large enough to make the GP sensitive to nonlocality and thus to deviate from Drude's model prediction regarding the coupling angle [26]. Defining the coupling angle as the angle for which reflectivity reaches its lowest value, we define $\Delta\theta_i$ as the difference between the local and nonlocal coupling angle—the nonlocal angle being always the smallest. To reach a meaningful difference, we have to push the GP wave vector as high as possible by using the smallest dielectric thickness. We are, however, limited by the prism refractive index which determines the maximum reachable effective index. That is the reason why we consider TiO_2 [44] prisms: they present the highest possible refractive index in the visible range and are commercially available.

We use Au as metal and air as dielectric (a setup for which the gap can thus be changed progressively). Figure 2 shows how, when the gap is decreased, the two interfaces become coupled, and the entrance in the GP regime when the effective index of the symmetric mode, and thus the angle of excitation, increase clearly compared to the surface plasmons. We stress that, when the interfaces are decoupled, the discrepancy

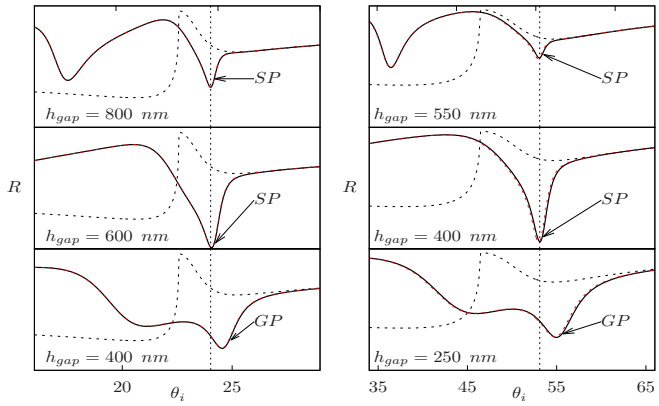

(a) gap = Air, $\lambda = 600$ nm **(b)** gap = LASF9, $\lambda = 750$ nm

FIG. 2. (a) Reflectivity in the local approximation (solid black line) and with the hydrodynamic model (dashed red line) for the MIM structure with air. The dashed black line corresponds to the coupler without the second metallic interface. The vertical dotted line shows where the undisturbed surface plasmon is expected. For large gaps, only the surface plasmon on the lower interface is excited. For the thinner gap, the symmetric and antisymmetric modes can clearly be seen. The angle of excitation for the symmetric mode is higher than for the SP, signaling the gap-plasmon regime. (b) Same situation with a dielectric loaded gap and a lower frequency. The impact of nonlocality begins to be noticeable because the resonance is at larger incidence angle.

between the local and the nonlocal descriptions is below 0.01°, a result coherent with previous studies of the phenomenon [10].

Figure 3—the reflectivity of our structure as a function of the incident angle for a wavelength λ of 600 nm. With $h_{\text{gap}} = 13.75$ nm (see left part of Fig 3), nonlocality causes a shift of the coupling angle of more than 1°, which is a two orders of magnitude increase compared to the surface

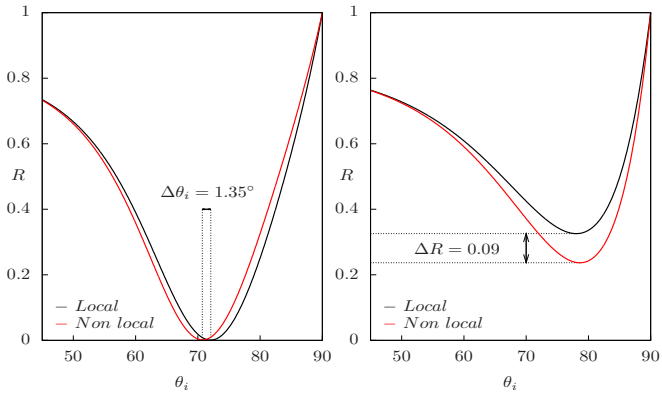

(a) $h_{gap} = 13.75$ nm **(b)** $h_{gap} = 11.50$ nm

FIG. 3. Reflectivity of the structure shown in Fig. 1(a) as a function of the incident angle θ_i for two values of h_{gap}. The wavelength of the incident light is $\lambda = 600$ nm. The prism is made of TiO_2 with a permittivity $\epsilon_p = 6.78$, the metal is Au with a permittivity $\epsilon_m = -8.44 + 1.41i$, and the dielectric is air. The upper metallic layer thickness is $h_c = 18$ nm. The resonance corresponds to the excitation of a gap plasmon.

plasmon. Here, the position of the reflectivity minimum is close to the coupling angle that can be determined from the dispersion relation—a regime that we thus call the plain coupling regime and for which the effective index of the mode is lower than the prism index.

For a slightly thinner gap ($h_{\text{gap}} = 11.50$ nm), the GP wave vector is beyond the maximum incident wave vector reachable but near enough to still impact the reflectivity. The reflectivity still presents a minimum, but its position cannot be predicted using the effective index of the mode anymore. The presence of the guided mode, even if it can be only imperfectly coupled, is still responsible for the minimum. We attribute the difference between Drude's model prediction and the predictions of the hydrodynamic model to the fact that the effective index of the GP is always lower when spatial dispersion is taken into account. The resonance being further off with a local description, the minimum is higher, while the presence of a closer resonance in the nonlocal case makes the minimum lower. This situation, that we call the near coupling regime, gives rise to a discrepancy ΔR for the minimum of the reflectivity, shown in Fig. 3. Such a difference appears at grazing incidence, but it may eventually be easier to measure than the angular shift in the plain coupling regime.

For both regimes, the only condition we have to satisfy to study nonlocality is to reach a high-enough wave vector for the GP. We have done this so far by using an extremely thin gap filled with air, but we now show it is possible to reach similar sensitivity to nonlocality relying on much larger thicknesses, provided the refractive index of the dielectric is significantly higher than 1.

For a fixed wavelength, using such materials actually leads plasmonic guided modes to present higher wave vectors than using air as dielectric for the same gap width. Very similar results to the above ones are obtained for much larger thicknesses of more than 60 nm. We have studied the case of a dielectric waveguide filled with LASF9 at a wavelength of $\lambda = 750$ nm. Exactly as previously, the impact of spatial dispersion is observed in the plain coupling regime, producing a shift of the coupling angle [see Fig. 4(a)], and in the near coupling regime [see Fig. 4(b)], producing a very large discrepancy in the reflectivity of 0.17. This setup presents several advantages as (i) it is probably easier to control the gap over macroscopic distances horizontally if it is filled with a dielectric, (ii) using a dielectric allows us to reach a higher effective index for quite large wavelengths, and (iii) such a large thickness allows us to completely neglect other phenomena like the spill-out, which intervene when extremely small gaps are involved.

Finally, we show that it is possible to excite the guided modes supported by the complementary structure: a metallic slab [19,41] buried in a dielectric, a structure we will call IMI shown in Fig. 1(b). We underline that the modes of a single metallic slab have been envisaged a long time ago in the framework of EELS [45]. Compared to the MIM structure, the IMI is able to support not only one but two guided modes, the LRSP and the SRSP. These two modes have two distinct wave vectors, which behave differently when the thickness of the metallic slab supporting them varies. The dispersion relation for the symmetric SRSP mode can be

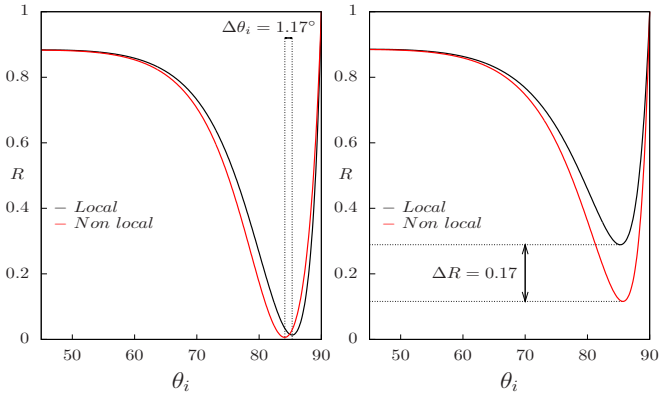

(a) $h_{gap} = 63.25$ nm **(b)** $h_{gap} = 60.00$ nm

FIG. 4. Reflectivity of the structure shown in Fig. 1(a) as a function of the incident angle θ_i for two values of h_{gap}. The wavelength of the incident light is $\lambda = 750$ nm. The prism is made of TiO_2 with a permittivity $\epsilon_p = 6.41$, the metal is Au with a permittivity $\epsilon_m = -18.50 + 1.50i$, and the dielectric is LASF9 with a permittivity $\epsilon_d = 3.37 + 1.10e^{-07}i$. The thickness of the upper metallic layer is $h_c = 18$ nm.

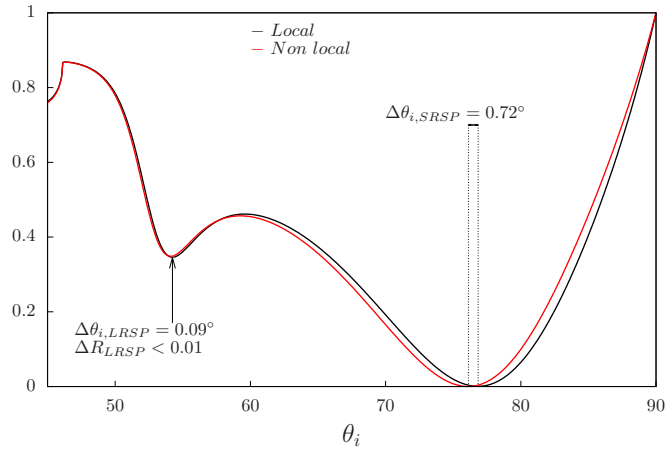

FIG. 5. Reflectivity of the structure shown in Fig. 1(b) as a function of the incident angle θ_i for $h_m = 44$ nm. The wavelength of the incident light is $\lambda = 700$. Prism is TiO_2 with permittivity $\epsilon_p = 6.50$, metal is Au with permittivity $\epsilon_m = -15.04 + 1.31i$, and dielectric is LASF9 with permittivity $\epsilon_d = 3.28 + 1.15 \times 10^{-07}i$ (a permittivity very close to one of the other high index dielectrics like Al_2O_3). The thickness of the layer under the prism is $h_c = 65$ nm. The two dips are due to the excitation of LRSP (left) in the plain regime and SRSP (right) in the near coupling regime.

written

$$\frac{\kappa_m}{\epsilon_m}\tanh\frac{\kappa_m h}{2} + \frac{\kappa_d}{\epsilon_d} = \Omega, \tag{4}$$

and for the antisymmetric LRSP,

$$\frac{\kappa_m}{\epsilon_m}\coth\frac{\kappa_m h}{2} + \frac{\kappa_d}{\epsilon_d} = \Omega. \tag{5}$$

As a consequence, while the SRSP tends to behave as the GP, i.e., to present a diverging wave vector when h_m tends to zero, the LRSP has a lower wave vector, which stays much more stable when h_m decreases. The reflectivity of our IMI structure excited through the prism thus presents two dips for two different angles corresponding, respectively, to the LRSP and SRSP modes. Here too the parameter Ω appears in the dispersion relation. Since it is larger when the wave vector k_x is larger, the impact of spatial dispersion can be expected to be much lower for the LRSP than for the SRSP [19,41]. Figure 5 shows that while spatial dispersion has a small impact on the LRSP, there is a clear shift of 0.72° for the higher effective index SRSP when nonlocality is taken into account. We underline that for such a setup the LRSP can thus be used to retrieve the material and geometrical parameters while the SRSP allows for a measurement of β.

In conclusion, we have shown how feasible multilayered structures could be used to enhance the impact of spatial dispersion in metals, through the excitation of three of the most emblematic guided mode in plasmonics: the GP, the SRSPs, and LRSPs. Physically, this enhancement by two orders of magnitude can be directly linked to the high wave vectors these plasmonic guided modes present. It is obtained here for dielectric gaps whose typical thicknesses, ranging from 10 nm to 70 nm, are one to two orders of magnitude larger than in previous experiments [15,16]. This allows us to rule out any role of more complex phenomena like the spill-out of the electron gas outside of the metal [21–23,33] because of the finite extraction work.

The geometrical parameters for which such strong nonlocal effects can be found suggest spatial dispersion has probably to be taken into account in plasmonics for much larger structures than previously thought. We underline that the present setups do not involve a large number of chemically synthesized nanoparticles [15,16,18,46] and, furthermore, that the working wavelengths are in the red part of the optical spectrum—which shows that these effects manifest themselves even far below the plasma frequency of metals.

We hope our work will pave the way for well-controlled optical experiments to assess whether or not the hydrodynamic model is an accurate replacement for Drude's in plasmonics. Given the increasing number of devices relying on GP excitation in dielectric-filled gaps [34,36,47,48], such an evolution may be a necessity soon.

This work has been supported by the National Agency for Research, Project Physics of Gap-Plasmons No. ANR-13-JS10-0003.

[1] P. Drude, Ann. Phys. **306**, 566 (1900).
[2] R. Fuchs and K. L. Kliewer, Phys. Rev. B **3**, 2270 (1971).
[3] P. J. Feibelman, Phys. Rev. B **12**, 1319 (1975).
[4] A. Eguiluz and J. Quinn, Phys. Rev. B **14**, 1347 (1976).
[5] A. D. Boardman, *Electromagnetic Surface Modes* (Wiley, New York, 1982).

[6] N. Crouseilles, P. A. Hervieux, and G. Manfredi, Phys. Rev. B **78**, 155412 (2008).

[7] Y. Wang, E. Plummer, and K. Kempa, Adv. Phys. **60**, 799 (2011).

[8] A. Liebsch, Phys. Rev. B **48**, 11317 (1993).

[9] A. Liebsch, Phys. Rev. Lett. **71**, 145 (1993).

[10] R. Chang, H.-P. Chiang, P. Leung, and W. Tse, Opt. Commun. **225**, 353 (2003).

[11] M. Rocca, Surf. Sci. Rep. **22**, 1 (1995).

[12] M. Rocca, Li Yibing, F. Buatier de Mongeot, and U. Valbusa, Phys. Rev. B **52**, 14947 (1995).

[13] S. J. Park and R. E. Palmer, Phys. Rev. Lett. **102**, 216805 (2009).

[14] F. Frostmann and R. R. Gerhardts, *Metal Optics near the Plasma Frequency*, Vol. 109 (Springer-Verlag, 1986).

[15] C. Ciracì, R. Hill, J. Mock, Y. Urzhumov, A. Fernández-Domínguez, S. Maier, J. Pendry, A. Chilkoti, and D. Smith, Science **337**, 1072 (2012).

[16] C. Ciracì, X. Chen, J. J. Mock, F. McGuire, X. Liu, S.-H. Oh, and D. R. Smith, Appl. Phys. Lett. **104**, 023109 (2014).

[17] C. Ciraci, J. B. Pendry, and D. R. Smith, Chem. Phys. Chem. **14**, 1109 (2013).

[18] J. A. Scholl, A. L. Koh, and J. A. Dionne, Nature **483**, 421 (2012).

[19] S. Raza, T. Christensen, M. Wubs, S. I. Bozhevolnyi, and N. A. Mortensen, Phys. Rev. B **88**, 115401 (2013).

[20] G. Hajisalem, Q. Min, R. Gelfand, and R. Gordon, Opt. Express **22**, 9604 (2014).

[21] R. Esteban, A. G. Borisov, P. Nordlander, and J. Aizpurua, Nat. Commun. **3**, 825 (2012).

[22] K. J. Savage, M. M. Hawkeye, R. Esteban, A. G. Borisov, J. Aizpurua, and J. J. Baumberg, Nature **491**, 574 (2012).

[23] T. V. Teperik, P. Nordlander, J. Aizpurua, and A. G. Borisov, Phys. Rev. Lett. **110**, 263901 (2013).

[24] A. I. Fernández-Domínguez, S. A. Maier, and J. B. Pendry, Phys. Rev. Lett. **105**, 266807 (2010).

[25] A. Wiener, A. I. Fernández-Domínguez, A. P. Horsfield, J. B. Pendry, and S. A. Maier, Nano Lett. **12**, 3308 (2012).

[26] A. Moreau, C. Ciracì, and D. R. Smith, Phys. Rev. B **87**, 045401 (2013).

[27] M. Dechaux, P.-H. Tichit, C. Ciracì, J. Benedicto, R. Pollès, E. Centeno, D. R. Smith, and A. Moreau, Phys. Rev. B **93**, 045413 (2016).

[28] G. Toscano, S. Raza, A.-P. Jauho, N. A. Mortensen, and M. Wubs, Opt. Express **20**, 4176 (2012).

[29] J. Benedicto, R. Pollès, C. Ciracì, E. Centeno, D. R. Smith, and A. Moreau, JOSA A **32**, 1581 (2015).

[30] N. Schmitt, C. Scheid, S. Lanteri, A. Moreau, and J. Viquerat, J. Comput. Phys. **316**, 396 (2016).

[31] H. Haberland, Nature **494**, E1 (2013).

[32] G. Toscano, J. Straubel, A. Kwiatkowski, C. Rockstuhl, F. Evers, H. Xu, N. A. Mortensen, and M. Wubs, Nat. Commun. **6**, 7132 (2015).

[33] C. Ciraci and F. Della Sala, Phys. Rev. B **93**, 205405 (2016).

[34] C. Haffner, W. Heni, Y. Fedoryshyn, J. Niegemann, A. Melikyan, D. L. Elder, B. Baeuerle, Y. Salamin, A. Josten, U. Koch, C. Hoessbacher, F. Ducry, L. Juchli, A. Emboras, D. Hillerkuss, M. Kohl, L. R. Dalton, C. Hafner, and J. Leuthold, Nat. Photonics **9**, 525 (2015).

[35] R. Smaali, F. Omeis, A. Moreau, E. Centeno, and T. Taliercio, Phys. Rev. B **95**, 155306 (2017).

[36] G. M. Akselrod, C. Argyropoulos, T. B. Hoang, C. Ciracì, C. Fang, J. Huang, D. R. Smith, and M. H. Mikkelsen, Nat. Photonics **8**, 835 (2014).

[37] T. Lopez-Rios, F. Abelès, and G. Vuye, J. Phys. Lett. **40**, 343 (1979).

[38] S. I. Bozhevolnyi and T. Søndergaard, Opt. Express **15**, 10869 (2007).

[39] P. Berini, Adv. Opt. Photonics **1**, 484 (2009).

[40] P. Berini, Phys. Rev. B **61**, 10484 (2000).

[41] A. Pitelet, E. Mallet, E. Centeno, and A. Moreau, Phys. Rev. B **96**, 041406 (2017).

[42] A. D. Rakic, A. B. Djurišic, J. M. Elazar, and M. L. Majewski, Appl. Opt. **37**, 5271 (1998).

[43] J. Defrance, C. Lemaître, R. Ajib, J. Benedicto, E. Mallet, R. Pollès, J.-P. Plumey, M. Mihailovic, E. Centeno, C. Ciracì, D. Smith, and A. Moreau, J. Open Res. Software **4**, e13 (2016).

[44] J. R. DeVore, J. Opt. Soc. Am. **41**, 416 (1951).

[45] R. Ritchie and H. Eldridge, Phys. Rev. **126**, 1935 (1962).

[46] S. Raza, S. I. Bozhevolnyi, M. Wubs, and N. A. Mortensen, J. Phys.: Condens. Matter **27**, 183204 (2015).

[47] J. B. Lassiter, X. Chen, X. Liu, C. Ciracì, T. B. Hoang, S. Larouche, S.-H. Oh, M. H. Mikkelsen, and D. R. Smith, Acs Photonics **1**, 1212 (2014).

[48] M. P. Nielsen, X. Shi, P. Dichtl, S. A. Maier, and R. F. Oulton, Science **358**, 1179 (2017).